Dyes and Pigments 171 (2019) 107715

Contents lists available at ScienceDirect

Dyes and Pigments

journal homepage: www.elsevier.com/locate/dyepig

A water-soluble cyclometalated iridium(III) complex with fluorescent sensing capability for hypochlorite

Zhen Lu[a,1], Mingqin Shangguan[a,1], Xingzong Jiang[a], Peiyao Xu[b], Linxi Hou[a,*], Tao Wang[c,**]

[a] College of Chemical Engineering, Fuzhou University, Xueyuan Road No. 2, Fuzhou, 350116, China
[b] College of Chemical Engineering, Huaqiao University, Xiamen, 361021, China
[c] Pediatric Department of Fujian Provincial Hospital, Fuzhou, Fujian, 350001, China

ARTICLE INFO

Keywords:
Fluorescent probe
Iridium(III) complex
Hypochlorite
Cell imaging

ABSTRACT

Herein, a novel cyclometalated iridium (III) complex (**Ir-1**) with good water-solubility was designed and synthesized to sensitively detect hypochlorite (ClO^-) in aqueous buffer solution. The sensor **Ir-1** was prepared by incorporating a methacrylate group into cyclometalated ligands, which was a specific response site toward ClO^- through an oxidation process. **Ir-1** displayed strong emission at 615 nm, while significant fluorescence quenching was observed upon addition of ClO^- with a low detection limit of 0.41 μM. Moreover, probe **Ir-1** exhibited a rapid response (< 30 s) for ClO^- with high selectivity over potentially competing species. The sensing process was evidenced by NMR and MS characterization. Further application in bioimaging of ClO^- was successfully performed in living HepG2 cells.

1. Introduction

Hypochlorous acid (HClO)/hypochlorite (ClO^-) is considered as a type of reactive oxygen species (ROS), generated predominantly from peroxidation reaction both hydrogen peroxide and chloride ions with the mediation of myeloperoxidase (MOP) enzyme during the process of cellular aerobic metabolism [1,2]. As one of the crucial members of ROS, maintaining the normal concentration of ClO^- in living cells takes more important role in building powerful biological immune systems to against inflammation and pathema [3,4]. However, abnormal concentration of ClO^- production in living cell may lead to damage of cellular morphology and cause harm to physiology, even cause a variety of diseases such as cardiovascular disease, nephropathy, and cancers [5,6]. Thus, it's necessary to develop a sensitive and selective detection method for monitoring the concentration of ClO^- in living cells at real-time, which could provide an accurate guidance for revealing its physiological functions.

Fluorescence spectrophotometric analysis has become an indispensable technique for the determination of many ions in vivo and in vitro owing to its outstanding sensitivity and selectivity, rapid response and convenient processes [7,8]. So far, fluorescent probes, such as the derivate of fluorescein [9], coumarin [10], rhodamine [11], BODIPY [12] and tetraphenylethylene [13], have been successfully developed and applied for detection ClO^- based on the specific responsive moieties, including C═N moiety [14], C═C moiety [15–17], oxime [18] and other response groups [19–22]. However, those organic dye-based fluorescent probes often encounter problems in actual application such as poor photobleaching resistance, low quantum yield, relative short emission wavelength and poor water solubility. Thus, there are still significant work to improve the fluorescent probes to promote their application.

Transition-metal complexes show distinct advantages for tackling the foregoing problems, for instance, their heavy atom effect on promoting the intersystem crossing (ISC) process, enhancing the quantum yield and extending the Strokes shift [23]. Meanwhile, relative long emission lifetimes can eliminate the autofluorescence of probe, which is significantly beneficial for fluorescent detection [24]. Among the various of transition-metal complexes, iridium (III) complexes are widely explored as fluorescent probe for detecting ROS in vivo and in vitro on account of their abundant and tunable ligand structures, large Stokes shift and high photo-stability, as well as prominent biocompatibility [25–28]. Combined with these advantages, iridium (III) complexes extend their application from sensing to cellular real-time monitoring and photodynamic therapy [29]. While conventional iridium (III) complexes suffered from poor water solubility, resulting in aggregation and reduction their sensing performance under aqueous solution.

* Corresponding author.
** Corresponding author.
E-mail addresses: lxhou@fzu.edu.cn (L. Hou), wangtao2003@126.com (T. Wang).
[1] The two authors contributed equally to this work.

https://doi.org/10.1016/j.dyepig.2019.107715
Received 4 June 2019; Received in revised form 13 July 2019; Accepted 13 July 2019
Available online 15 July 2019
0143-7208/

Usually, organic solvents such as CH_3CN and DMF are applied to increase the solubility of iridium (III) complexes in aqueous solution as co-solvents, while causes high toxicity to biological tissues [30]. To solve these problems, diverse methods have been developed, including incorporation of solubilising groups into ligands [28] and combination with either surfactants or soluble polymers [31–34].

In previous work, the modification of the quaternary ammonium groups on iridium (III) complexes not only endowed their water solubility but also tailored their fluorescent properties [35]. Inspired by our previous work, herein, we designed and synthesized a new cyclometalated iridium (III) complexes ClO^- probe (**Ir-1**), which includes two moieties: a water solubility auxiliary ligand (N^N) modified with quaternary ammonium groups and the response units attached into cyclometalated ligands (C^N). The C–O bonds in probe **Ir-1** exhibited specific cleavage by ClO^- and quench the fluorescence to "turn-off". The probe showed ultrasensitivity and accurate response toward ClO^- (detection limit was 0.41 μM) within short responses time (< 30 s). Based on the excellent sensitivity and selectivity for detecting ClO^- in vitro, we further investigated the ability to monitor ClO^- in cellular environment. The results indicated that **Ir-1** exhibits promising performance for detecting ClO^- in bio-system. In this contribution, we further expect that these modification methods will open a protocol for regulating the water solubility of transition metal complexes, which can be used in profound study around the biomedicine science area such as cell imaging, drug delivery and targeting therapy toward tumor.

2. Experimental

2.1. Materials and apparatus

All chemical materials and solvents were purchased commercially without further purification. ^{1}H NMR spectra of compounds were performed on a Bruker Avance III 500 MHz instrument. Mass spectra were recorded on Agilent HPLC-MS. Fluorescent spectra and UV–vis absorption spectra were determined on a Hitachi F-4600 spectrofluorometer and on a Lambda 750 UV–vis spectrophotometer. Fluorescent images were conducted with a Leica TCS SP8 Laser Scanning Confocal Microscope.

2.2. Synthesis and characterization

2.2.1. Synthesis of compound 1 (4-(pyridin-2-yl)phenyl methacrylate)

Sodium hydride (14 mg, 0.6 mmol) was added slowly to a solution of 2-(4-hydroxypenyl)pyridine (100 mg, 0.58 mmol) in THF (20 mL) while stirred at 0 °C for 30 min. Then, methacryloyl chloride (90 mg, 0.86 mmol) in THF (1 mL) was added into the solution for additional 6 h stirring at room temperature. The reaction mixture was quenched with water (20 mL) and extracted with ethyl acetate (20 mL) three times. The organic layer was dried over $MgSO_4$ and the solvent was removed. Finally, the crude product was purified by chromatography on silica gel using dichloromethane as eluent to obtain the product **1** (108 mg, 78%, yellow solid). ^{1}H NMR (500 MHz, $CDCl_3$) δ 8.66 (d, J = 4.6 Hz, 1H), 8.04 (s, 2H), 7.75 (d, J = 7.6 Hz, 1H), 7.28 (s, 4H), 6.97 (d, J = 8.7 Hz, 1H), 6.40 (s, 1H), 5.83–5.76 (m, 1H), 2.10 (s, 3H). HR-MS (ESI): m/z $[M+H]^+$ calcd for $C_{15}H_{14}NO_2$, 240.1019; found, 240.1013.

2.2.2. Synthesis of compound Ir-1

The auxiliary ligand (N^N) of iridium complex: compound **2** (4,4′-bis [(trimethylamino)methyl]-2,2′-bipyridine) was synthesized following the method previously reported [36,37]. The synthetic routes of the probe **Ir-1** was shown in Scheme 1.

$IrCl_3$ (58 mg, 0.18 mmol) and compound **1** (78 mg, 0.32 mmol) were poured into a flask including a solvent mixture of 2-ethoxyethanol (30 mL) and H_2O (10 mL). The mixture was heated at 125 °C with stirring for 24 h. After cooling to room temperature, reddish-orange compound **3** (cyclometalated iridium (III) chloro-bridge dimer) was obtained by filtration and washed with water and ether, which was used directly without further purification. Compound **3** (60 mg, 0.04 mmol) and auxiliary ligand compound **2** (35 mg, 0.08 mmol) were added into flask contained methanol (10 mL) and dichloromethane (20 mL) under reflux with stirring for 24 h. The reaction solution was evaporated under vacuum and subsequently a small quantity of water was added. Filtered to obtain final solution and evaporated the water under vacuum, the product **Ir-1** was acquired (31 mg, 80%, red solid). ^{1}H NMR (500 MHz, D_2O) δ 8.78 (d, J = 5.1 Hz, 2H), 8.25 (dd, J = 36.6, 7.3 Hz, 4H), 8.03 (d, J = 7.9 Hz, 2H), 7.88 (d, J = 4.4 Hz, 2H), 7.67 (d, J = 3.8 Hz, 4H), 7.64–7.56 (m, 2H), 7.50 (d, J = 6.0 Hz, 2H), 7.00 (d, J = 6.4 Hz, 2H), 6.83 (d, J = 8.5 Hz, 2H), 6.15 (s, 2H), 4.61 (s, 4H), 3.15 (s, 19H), 1.85 (s, 6H). HR-MS (ESI): m/z^{2+} $[M]^{2+}$ calcd for $C_{48}H_{52}N_6O_4Ir$, 484.6901; found, 484.6813.

2.3. Spectroscopic measurements

Spectrophotometric titrations of the probe **Ir-1** were investigated in aqueous solution containing PBS (10 mM, pH = 7.4). The testing solutions of various species (NaClO, H_2O_2, GSH, NO_2^-, NO_3^-, SO_4^{2-}, SO_3^{2-}, Fe^{3+}, Cu^{2+}, F^-, Br^-, $ONOO^-$, •OH, $•O_2^-$) were prepared in deionized water. For fluorescence titration experiment, the excitation wavelength was 370 nm with slit widths at 5 nm.

2.4. Cytotoxicity assay

The toxicity of probe **Ir-1** toward HepG2 cells was evaluated through MTT (3-(4,5-dimethyl-2-thiazolyl)-2,5-diphenyl-2-H-tetrazolium bromide) assays. 96-well plates were used to seed cells at a concentration of 5×10^3 cells per well and the cells were incubated in an incubator (37 °C, 5% CO_2) for 24 h. The cells were further cultivated for another 24 h after treated with a series of different concentrations of probes (0,10,20,30 and 40 μM). MTT solution was then added into plates and the cells were cultured for another 4 h. Before the addition of 150 μL DMSO, the residual MTT solution was discarded. The absorbance of separated well was measured using a microplate reader (Varioskan Flash 1510, Thermo Fisher Scientific, Finland) at the wavelength of 490 nm. Cells viability rates were obtained according to the following equation: Cell viability (%) = (mean Abs. of treatment group/mean Abs. of control) × 100.

2.5. Cell imaging of probe Ir-1

HepG2 cells were cultivated under a humid atmosphere containing 5% CO_2 at 37 °C for 24 h in Dulbecco's modified Eagle's medium (DMEM) with 10% FBS fetal bovine serum (FBS). The well-grown cells were pretreated with probe **Ir-1** (10 μM) for 30 min and the residual probes were washed with PBS buffer for 3 times. Several plates were incubated for extra 10 min after adding ClO^- (50 μM), and the HepG2 cells were washed by PBS before imaging. Cell imaging were recorded with a laser scanning confocal microscope. The excitation wavelength was fixed at 405 nm.

2.6. Determination of quantum yield

Fluorescent quantum yield (QY) was determined using an aqueous solution of $[Ru(bpy)_3]Cl_2$ (QY = 0.028) as a reference by optically dilute method. The quantum yield was calculated from the following equation: $\Phi_f = (A_r I_f / A_f I_r) \times \Phi_r$, where Φ_f and Φ_r are quantum yield of sample and that of the reference respectively; I_f and I_r are the integrated areas of emission bands, A_f and A_r are the absorbance of the sample and the reference.

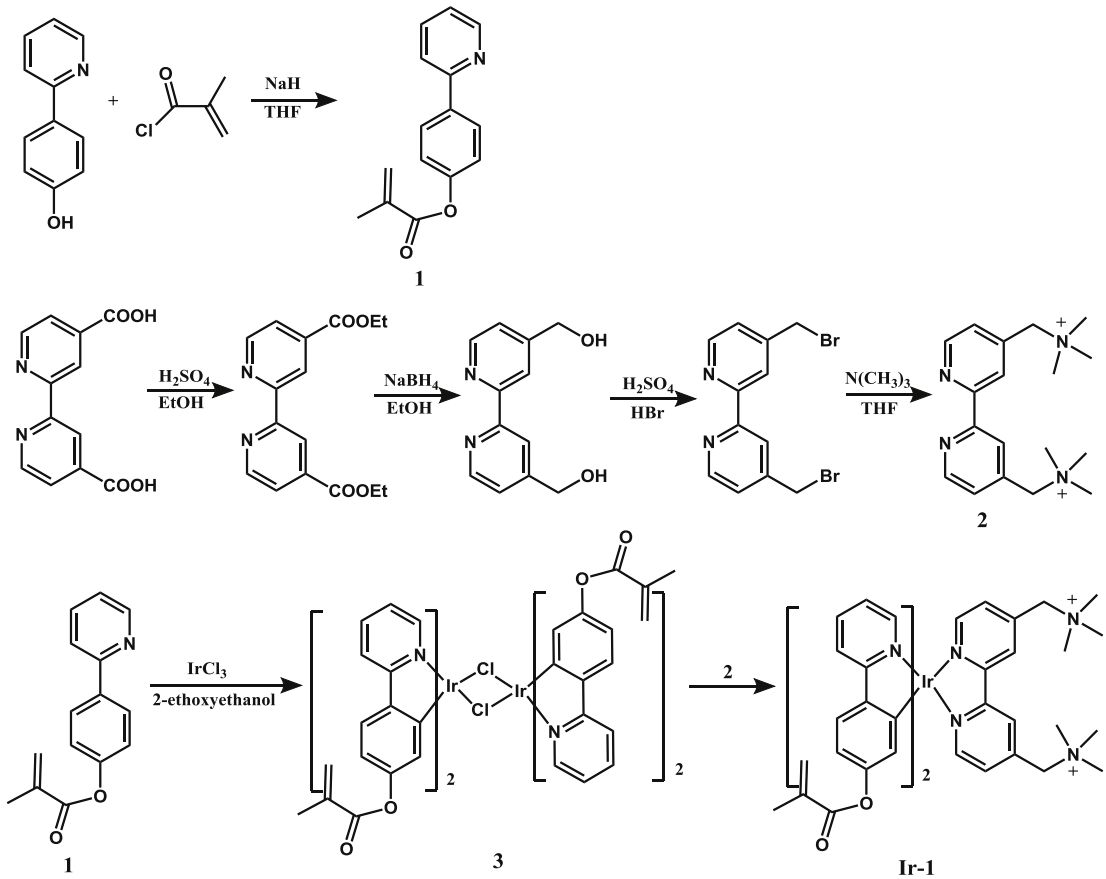

Scheme 1. Synthetic routes of the probe **Ir-1**.

3. Results and discussion

3.1. Design and synthesis of probe Ir-1

In order to develop a water-soluble fluorescent probe for ClO^-, **Ir-1** was designed and synthesized according to the routes displayed in Scheme 1. Iridium (III) complex was designed as fluorophore due to its outstanding photophysical properties. The methacrylate group was modified into the cyclometalated ligand as the response site. Through introducing a quaternary ammonium group into the auxiliary ligand, detection of ClO^- in 100% aqueous media could be achieved. A cyclometalated iridium (III) complex-based fluorescent probe **Ir-1** was successfully synthesized with thesis consideration. All compounds were confirmed by HPLC-MS and NMR.

3.2. Photophysical property studies

The fluorescent response of probe **Ir-1** upon addition of ClO^- was first explored by titrimetric spectra analysis. As illustrated in Fig. 1A, a strong reddish-orange emission was observed at about 615 nm with the quantum yield (Φ_{f1}) of 0.089. Upon the addition of ClO^-, **Ir-1** displayed an obvious fluorescence quenching response and the quantum yield (Φ_{f2}) was decreased to 0.011. The relationship between fluorescent intensity ratio (F/F_0) and increased concentration of ClO^- was depicted in Fig. 1B. As envision, the maximum fluorescent intensity of **Ir-1** could be reduced by 87% until exposure to 90 μM ClO^- solution. Furthermore, the relationship of F/F_0 versus ClO^- concentration within the range from 0 to 80 μM showed an excellent linearity with high coefficient ($R^2 = 0.997$) (inset in Fig. 1B). Subsequently, the limit of detection (D) for ClO^- was estimated to be as low as 0.41 μM based on the equation: $D = 3\sigma/k$ [38,39]. The above results demonstrated that **Ir-1** was sufficiently sensitive for practical analysis of ClO^-. Meanwhile, the UV–vis absorption spectra of **Ir-1** before and after addition of ClO^- were carried out. As shown in Fig. 2, the absorption peak of **Ir-1** increased at 255–355 nm, which should be attributed to the cleavage of C–O bonds in the cyclometalated primary ligands of **Ir-1**. Additionally, upon the addition of ClO^-, an obvious fluorescence quenching (from reddish-orange to colorless) was observed instantly under a 365 nm UV lamp (the inset of Fig. 2), allowing visual detection of ClO^- by the "naked-eye".

3.3. Effect of time and pH

To acquire a better understanding of response behavior, the effect of time was investigated by tracing the fluorescence changes. Fig. 3 showed that no visible variations for fluorescent intensity were observed in the absence of ClO^- even though the time was extended to 105 s, which suggested the stable of probe **Ir-1** in the assay condition. However, after addition of ClO^- (30, 50 and 80 μM, respectively), the fluorescent intensity decreased rapidly and then reached equilibrium within 30 s, which indicated that probe **Ir-1** could be used to facilitate real-time detection of ClO^-. The short response time was superior to most of reported fluorescent probes (listed in Table S1). In order to study the practical application, the pH effect on the fluorescent response of probe **Ir-1** toward ClO^- was performed with pH ranging from 1 to 12. As displayed in Fig. 4, it could be seen that the fluorescent intensities of probe **Ir-1** were not significantly changed over the relatively wide pH range of 5–9. Therefore, probe **Ir-1** could be suitable to detect ClO^- in biological systems.

3.4. Selectivity study

To assess the sensing specificity of **Ir-1** toward ClO^-, the changes of fluorescent intensity of **Ir-1** upon addition of some ROS species and

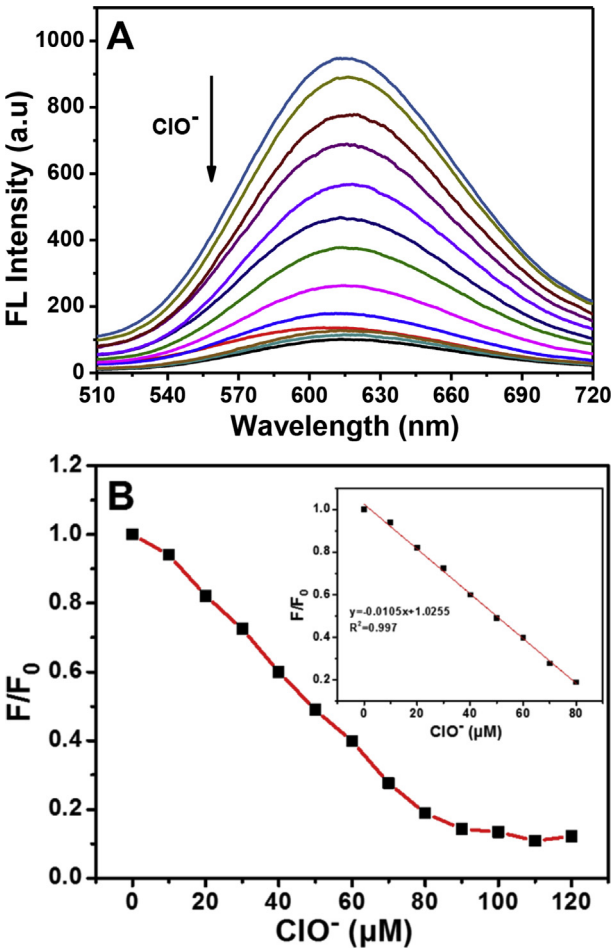

Fig. 1. (A) Fluorescent titration spectra of probe **Ir-1** (10 μM) in the presence of increasing amount of ClO^- (0–120 μM) in PBS solution (10 mM, pH 7.4), λ_{ex} = 370 nm. (B) Fluorescent intensity ratio (F/F_0) of the probe **Ir-1** (10 μM) in response to ClO^- concentrations (0–120 μM). The inset shows the linear relationship for the concentration of ClO^- (0–80 μM).

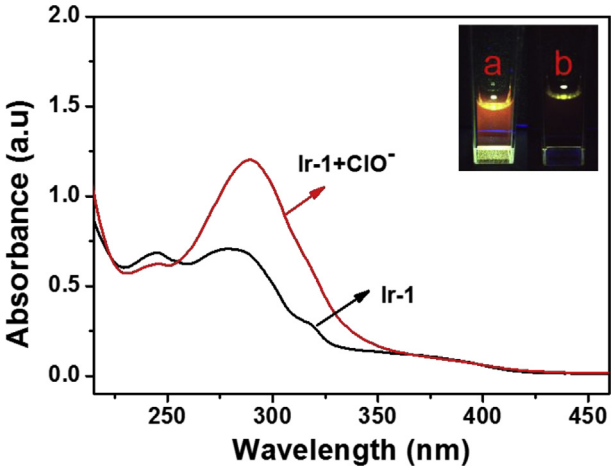

Fig. 2. UV–vis absorption spectra of **Ir-1** (10 μM) in the presence of ClO^- in PBS solution (10 mM, pH 7.4).

common ions were examined. As shown in Fig. 5A, the fluorescent intensity of **Ir-1** was quenched dramatically in the presence of ClO^- and could be barely affected by the addition of other relevant analytes, such as H_2O_2, GSH, NO_2^-, NO_3^-, SO_4^{2-}, SO_3^{2-}, Fe^{3+}, Cu^{2+}, F^-, Br^-, $ONOO^-$, •OH, $•O_2^-$. The result demonstrated that probe **Ir-1** displayed

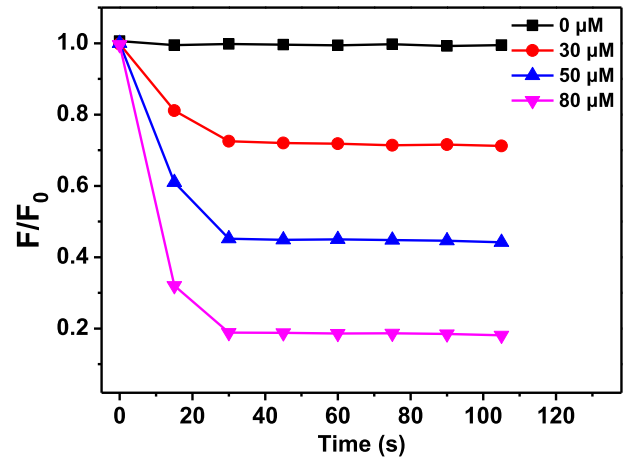

Fig. 3. Real-time responses of probe **Ir-1** (10 μM) with ClO^- (30, 50 and 80 μM) in PBS solution (10 mM, pH 7.4), λ_{ex} = 370 nm, λ_{em} = 615 nm.

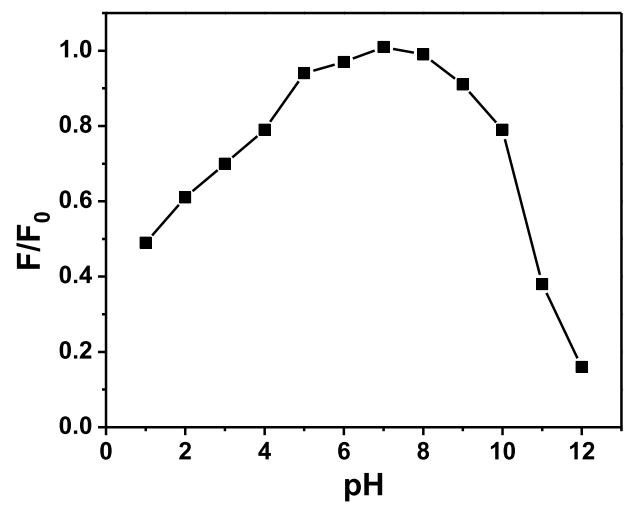

Fig. 4. Emission intensity ratio (F/F_0) of **Ir-1** (10 μM) under various pH values, λ_{ex} = 370 nm, λ_{em} = 615 nm.

a specific "turn-off" fluorescent response toward ClO^-. To further evaluate the selectivity, the competitive experiments were conducted by adding ClO^- to probe **Ir-1** solution containing aforementioned relevant analytes. From Fig. 5B, it can be seen that obvious fluorescence changes of **Ir-1** were observed with the addition of ClO^- even in the presence of interferential species. So we can conclude that probe **Ir-1** possesses a good selectivity with little interference, which is good for a real environment application.

3.5. Proposed sensing mechanism

Based on the strong oxidizing property and experimental results, a proposed sensing mechanism was shown in Scheme 2. To confirm the reaction mechanism between probe **Ir-1** and ClO^-, the ^1H NMR experiments were performed. As shown in Fig. S1, upon addition of ClO^-, a signal peak at 6.18 ppm corresponding to methacrylate group disappeared and a new signal peak at 9.30 ppm was presented, which was ascribed to the cleavage of C–O bonds by ClO^-. Additionally, the mass spectra were further conducted to investigate the sensing mechanism. The mass spectra of fluorescent product appeared a dominant peak at 415.6523 (m/z^{2+}) corresponding to the **IrOH** (Fig. S2). These results confirmed that a hydroxy group was generated accompanying the break of C–O bonds by ClO^-.

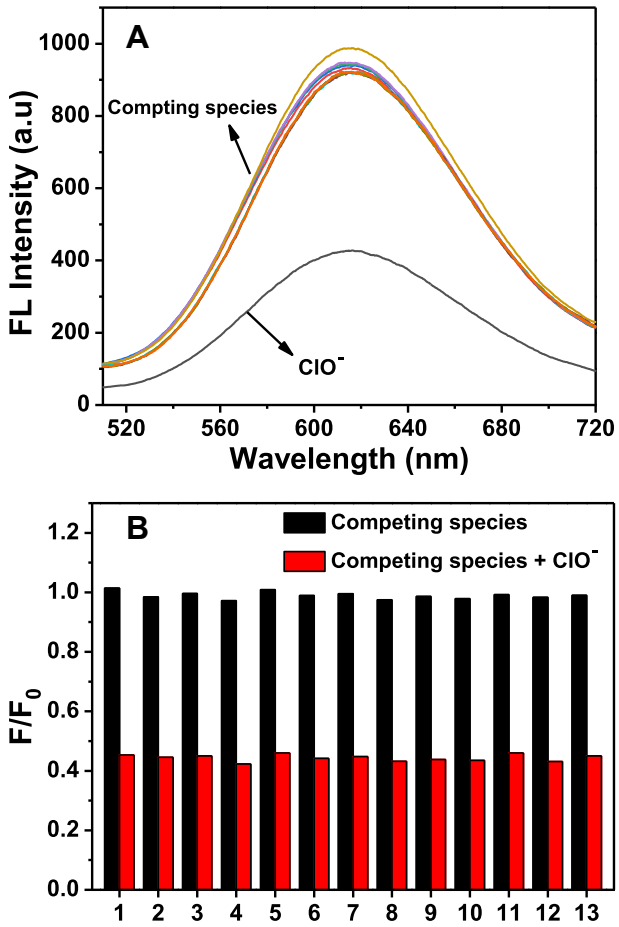

Fig. 5. (A) Fluorescent intensity of probe **Ir-1** (10 μM) in the presence of ClO^- and relevant analytes (50 μM); (B) Changes in emission intensity ratio of probe **Ir-1** (10 μM) with various competing species (50 μM) in response to ClO^- (1–13: H_2O_2, GSH, NO_2^-, NO_3^-, SO_4^{2-}, SO_3^{2-}, Fe^{3+}, Cu^{2+}, F^-, Br^-, $ONOO^-$, •OH, $•O_2^-$).

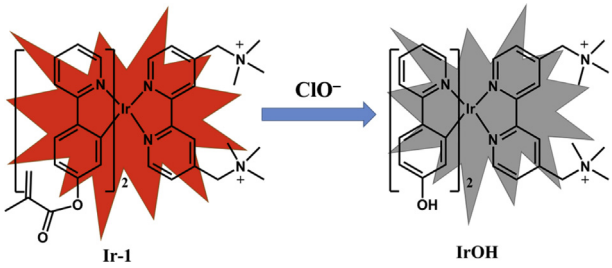

Scheme 2. Proposed reaction mechanism for ClO^-.

3.6. Cell imaging

The cytotoxicity of probe **Ir-1** toward HepG2 cells was firstly carried out by MTT assay. As shown in Fig. S3, the viability of HepG2 cells kept more than 90% after incubated with various concentration (0, 10, 20, 30, and 40 μM) of **Ir-1** for 24 h, which implied the low cytotoxicity of **Ir-1**. Accordingly, the application of **Ir-1** for fluorescent imaging for ClO^- in living cells was performed. After incubated with **Ir-1** for 30 min, HepG2 cells showed strong fluorescence (shown in Fig. 6). In contrast, after treated with ClO^- for another 10 min, a significant decrease in intracellular fluorescence was observed. These results indicated that **Ir-1** was biocompatible and able to display a fluorescent response toward ClO^- in living cells.

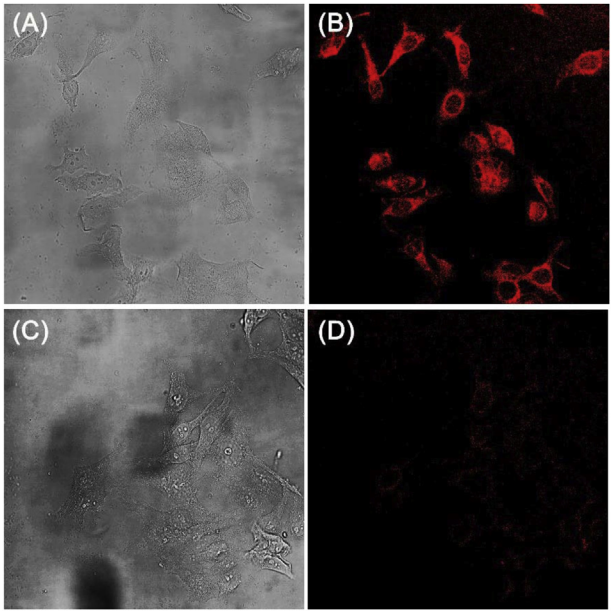

Fig. 6. Fluorescence images of HepG2 cells. (A, B) HepG2 cell incubated with **Ir-1** (10 μM) and (C, D) **Ir-1** + ClO^- (50 μM); (A) and (C) are bright-field image; (B) and (D) are fluorescence image.

4. Conclusion

In conclusion, a iridium (III) complex based fluorescent probe (**Ir-1**) for ClO^- was presented by introducing a methacrylate group into the cyclometalated ligand as the recognition site. **Ir-1** could exhibited rapid response time and excellent selectivity for ClO^- over other interferential species in aqueous buffer solution. The sensing mechanism was verified by ^1H NMR spectra and HPLC-MS. In addition, **Ir-1** could realize the detection of ClO^- in living cells with excellent biocompatibility. Therefore, **Ir-1** provided a potential application for bioluminescence labeling in living systems.

Conflicts of interest

All the authors listed here declare that we have no conflict of interests.

Acknowledgements

This work was supported by the National Natural Science Foundation of China (No: 21676057), United Fujian Provincial Health and Education Project for Tackling the Key Research.P.R.China (WKJ2016-2-04) and Scientific Research Topics of Traditional Chinese Medicine in Fujian Provincial Department of Health (WZZY201317).

Appendix A. Supplementary data

Supplementary data to this article can be found online at https://doi.org/10.1016/j.dyepig.2019.107715.

References

[1] Wu L, Wu IC, DuFort CC, Carlson MA, Wu X, Chen L, Kuo CT, Qin Y, Yu J, Hingorani SR, Chiu DT. Photostable ratiometric pdot probe for in vitro and in vivo imaging of hypochlorous acid. J Am Chem Soc 2017;139:6911–8.
[2] Pak YL, Park SJ, Xu Q, Kim HM, Yoon J. Ratiometric two-photon fluorescent probe for detecting and imaging hypochlorite. Anal Chem 2018;90:9510–4.
[3] Kang J, Huo F, Yue Y, Wen Y, Chao J, Zhang Y, Yin C. A solvent depend on ratiometric fluorescent probe for hypochlorous acid and its application in living cells. Dyes Pigments 2017;136:852–8.
[4] Ma P, Zhang B, Diao Q, Li L, Sun Y, Wang X, Song D. A water-soluble fluorescent

probe for ClO^- and Cd^{2+} under physiological pH and its applications in living cells imaging. Sens Actuators, B 2016;233:639–45.
[5] Zhu B, Wu L, Zhang M, Wang Y, Liu C, Wang Z, Duan Q, Jia P. A highly specific and ultrasensitive near-infrared fluorescent probe for imaging basal hypochlorite in the mitochondria of living cells. Biosens Bioelectron 2018;107:218–23.
[6] Zhu B, Wu L, Zhang M, Wang Y, Liu C, Wang Z, Duan Q, Jia P. A highly specific and ultrasensitive near-infrared fluorescent probe for imaging basal hypochlorite in the mitochondria of living cells. Biosens Bioelectron 2018;107:218–23.
[7] Lee MH, Kim JS, Sessler JL. Small molecule-based ratiometric fluorescence probes for cations, anions, and biomolecules. Chem Soc Rev 2015;44:4185–91.
[8] Ren M, Zhou K, He L, Lin W. Mitochondria and lysosome-targetable fluorescent probes for HOCl: recent advances and perspectives. J Mater Chem B 2018;6:1716–33.
[9] Ren M, Li Z, Nie J, Wang L, Lin W. A photocaged fluorescent probe for imaging hypochlorous acid in lysosomes. Chem Commun 2018;54:9238–41.
[10] Zhang Q, Zhu Z, Zheng Y, Cheng J, Zhang N, Long Y-T, Zheng J, Qian X, Yang Y. A three-channel fluorescent probe that distinguishes peroxynitrite from hypochlorite. J Am Chem Soc 2012;134:18479–82.
[11] Shen S-L, Zhao X, Zhang X-F, Liu X-L, Wang H, Dai Y-Y, Miao J-Y, Zhao B-X. A mitochondria-targeted ratiometric fluorescent probe for hypochlorite and its applications in bioimaging. J Mater Chem B 2017;5:289–95.
[12] Shen B-x, Qian Y, Qi Z-q, Lu C-g, Sun Q, Xia X, Cui Y-p. Near-infrared BODIPY-based two-photon ClO^- probe based on thiosemicarbazide desulfurization reaction: naked-eye detection and mitochondrial imaging. J Mater Chem B 2017;5:5854–61.
[13] Dong X, Zhang G, Shi J, Wang Y, Wang M, Peng Q, Zhang D. A highly selective fluorescence turn-on detection of ClO^- with 1-methyl-1,2-dihydropyridine-2-thione unit modified tetraphenylethylene. Chem Commun 2017;53:11654–7.
[14] Qiao L, Nie H, Wu Y, Xin F, Gao C, Jing J, Zhang X. An ultrafast responsive BODIPY-based fluorescent probe for the detection of endogenous hypochlorite in live cells. J Mater Chem B 2017;5:525–30.
[15] Gu J, Li X, Zhou Z, Liao R, Gao J, Tang Y, Wang Q. Synergistic regulation of effective detection for hypochlorite based on a dual-mode probe by employing aggregation induced emission (AIE) and intramolecular charge transfer (ICT) effects. Chem Eng J 2019;368:157–64.
[16] Zhou Z, Gu J, Qiao X, Wu H, Fu H, Wang L, Li H, Ma L. Double protected lanthanide fluorescence core@shell colloidal hybrid for the selective and sensitive detection of ClO^-. Sens Actuators, B 2019;282:437–42.
[17] Zhu H, Fan J, Wang J, Mu H, Peng X. An "enhanced PET"-based fluorescent probe with ultrasensitivity for imaging basal and elesclomol-induced HClO in cancer cells. J Am Chem Soc 2014;136:12820–3.
[18] Reja SI, Bhalla V, Sharma A, Kaur G, Kumar M. A highly selective fluorescent probe for hypochlorite and its endogenous imaging in living cells. Chem Commun 2014;50:11911–4.
[19] Wu L, Yang Q, Liu L, Sedgwick AC, Cresswell AJ, Bull SD, Huang C, James TD. ESIPT-based fluorescence probe for the rapid detection of hypochlorite (HOCl/ClO^-). Chem Commun 2018;54:8522–5.
[20] Yuan L, Wang L, Agrawalla BK, Park SJ, Zhu H, Sivaraman B, Peng J, Xu QH, Chang YT. Development of targetable two-photon fluorescent probes to image hypochlorous acid in mitochondria and lysosome in live cell and inflamed mouse model. J Am Chem Soc 2015;137:5930–8.
[21] Huo B, Du M, Shen A, Li M, Lai Y, Bai X, Gong A, Fang L, Yang Y. A "light-up" fluorescent probe based on TEMPO-oxidation for the detection of ClO^- and application in real samples. Sens Actuators, B 2019;284:23–9.
[22] Ren M, Zhou K, He L, Lin W. Mitochondria and lysosome-targetable fluorescent probes for HOCl: recent advances and perspectives. J Mater Chem B 2018;6:1716–33.
[23] McKenzie LK, Sazanovich IV, Baggaley E, Bonneau M, Guerchais V, Williams JAG, Weinstein JA, Bryant HE. Metal complexes for two-photon photodynamic therapy: a cyclometallated iridium complex induces two-photon photosensitization of cancer cells under near-IR light. Chem-Eur J 2017;23:234–8.
[24] You Y, Lee S, Kim T, Ohkubo K, Chae WS, Fukuzumi S, Jhon GJ, Nam W, Lippard SJ. Phosphorescent sensor for biological mobile zinc. J Am Chem Soc 2011;133:18328–42.
[25] Zhang Y, Zhao M, Chao D. A cyclometalated iridium(III) complex for selective luminescent detection of hydrogen sulfide. Sens Actuators, B 2017;248:19–23.
[26] Li G, Lin Q, Ji L, Chao H. Phosphorescent iridium(III) complexes as multicolour probes for imaging of hypochlorite ions in mitochondria. J Mater Chem B 2014;2:7918–26.
[27] Lin S, Wang W, Hu C, Yang G, Ko C-N, Ren K, Leung C-H, Ma D-L. The application of a G-quadruplex based assay with an iridium(iii) complex to arsenic ion detection and its utilization in a microfluidic chip. J Mater Chem B 2017;5:479–84.
[28] Zhang KY, Zhang T, Wei H, Wu Q, Liu S, Zhao Q, Huang W. Phosphorescent iridium (iii) complexes capable of imaging and distinguishing between exogenous and endogenous analytes in living cells. Chem Sci 2018;9:7236–40.
[29] Zhao Q, Huang C, Li F. Phosphorescent heavy-metal complexes for bioimaging. Chem Soc Rev 2011;40:2508–24.
[30] Li G, Lin Q, Sun L, Feng C, Zhang P, Yu B, Chen Y, Wen Y, Wang H, Ji L, Chao H. A mitochondrial targeted two-photon iridium(III) phosphorescent probe for selective detection of hypochlorite in live cells and in vivo. Biomaterials 2015;53:285–95.
[31] Huang C, Ran G, Zhao Y, Wang C, Song Q. Synthesis and application of a water-soluble phosphorescent iridium complex as turn-on sensing material for human serum albumin. Dalton Trans 2018;47:2330–6.
[32] Meng X, Shi Y, Chen Z, Song L, Zhao M, Zou L, Liu S, Huang W, Zhao Q. Extending hypochlorite sensing from cells to elesclomol-treated tumors in vivo by using a near-infrared dual-phosphorescent nanoprobe. ACS Appl Mater Interfaces 2018;10:35838–46.
[33] Wang H, Zhao W, Zhou L, Wang J, Liu L, Wang S, Wang Y. Soft particles of gemini surfactant/conjugated polymer for enhanced anticancer activity of chemotherapeutics. ACS Appl Mater Interfaces 2018;10:37–41.
[34] Wang H, Zhou L, Zhou C, Zhao W, Wang J, Liu L, Wang S, Wang Y. Preparation of gemini surfactant/conjugated polymer aggregates for enhanced fluorescence and bioimaging application. ACS Appl Mater Interfaces 2017;9:23544–54.
[35] Yi S, Lu Z, Zhang J, Wang J, Xie Z, Hou L. Amphiphilic gemini iridium(III) complex as a mitochondria-targeted theranostic agent for tumor imaging and photodynamic therapy. ACS Appl Mater Interfaces 2019;11:15276–89.
[36] Swords WB, Li G, Meyer GJ. Iodide ion pairing with highly charged ruthenium polypyridyl cations in CH_3CN. Inorg Chem 2015;54:4512–9.
[37] Li J-H, Wang J-T, Hu P, Zhang L-Y, Chen Z-N, Mao Z-W, Ji L-N. Synthesis, structure and nuclease activity of copper complexes of disubstituted 2,2′-bipyridine ligands bearing ammonium groups. Polyhedron 2008;27:1898–904.
[38] Shangguan M, Jiang X, Lu Z, Zou W, Chen Y, Xu P, Pan Y, Hou L. A coumarin-based fluorescent probe for hypochlorite ion detection in environmental water samples and living cells. Talanta 2019;202:303–7.
[39] Wang Z, Zhang Y, Song J, Yang Y, Xu X, Li M, Xu H, Wang S. A novel isolongifolanone based fluorescent probe with super selectivity and sensitivity for hypochlorite and its application in bio-imaging. Anal Chim Acta 2019;1051:169–78.